An overview of PAF beamforming methods, and a novel beam modeling concept

Marianna V. Ivashina

VINNMER – FP7 Marie Curie International Qualification Fellowship for research on Antenna Systems for the next generation radio telescope – the SKA.

VINNMER grant is supported by part by:

- Department of Space and Earth Sciences (Chalmers) and
- The Netherlands Institute for Radio Astronomy (ASTRON).

CHALMERS

3GCII-Workshop, Portugal, September 23^{d}, 2011

Outline

- Part I: An overview of the PAF beamforming methods;

- Part II: A novel beam modeling concept:
  - Validation for AAs;
  - Initial results for PAFs.

Introduction:

- Early RA with reflector antennas:

The progress was driven by improvements in the hardware with relatively straightforward signal processing and detection techniques (*J. D. Kraus, 1986*);

- RA with large synthesis arrays:

- more complex signal processing algorithms (*Thompson, Moran, and Swenson, 2001*);

- Future RA with beamforming PAFs:

- opens a new frontier for both antenna design and signal processing developments.

PAF hardware developments

First R&D activities (since ~2000):

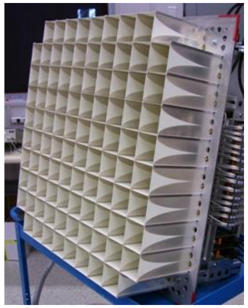

- NRAO/BYU: a 19-element array of sinuous antennas (*Fisher/Bradley, 2000*), dipole antennas (*Warnick/Jeffs, 2004*);

- ASTRON: wideband Vivaldi arrays (*Ivashina, Bregman 2002*);
- DRAO: a wideband Vivaldi array (*Veidt/Dewdney, 2006*);

- CSIRO: a wideband connected checkerboard array (*Hay/O'Sullivan, 2007*).

First PAF-equipped telescopes:

already in a few years from now: APERTIF, ASKAP;

More far future:

MeerKAT (?), SKA-Phase2 might/will be upgraded to a PAF implementation.

Development of the PAF BeamFormers (BFs):

- 2004-2008 — 1^{st} G BFs – a signal* model (including the array element mutual coupling), excitation-dependent noise coupling effects were ignored;
- 2008-2010 — 2^{nd} G BFs - the signal and noise models* (including the effect of element mutual coupling on both signal and noise response of the system), one polarization;
- Since 2010 — 3^{d} G BFs – extend to polarimetric BFs (for perfectly polarized and unpolarized reference calibration sources)
- Future — 4G BFs – interferometers,….

* a signal model describes the system response to a (point) source of interest on the sky; a noise model describes the system response to external (ground, sky) and internal (LNAs, ohmic loss) noise sources

1^{st}G PAF beamforming methods

- 2004-2008
  - the understanding of the PAF noise performance was limited;
  - accurate system models/tools were in process of development.

First methods optimized the shape of the antenna pattern by maximizing G/T for an assumed constant $T_{rec} \approx T_{lna}$
($\Rightarrow$ The excitation-dependent noise coupling effects were ignored)

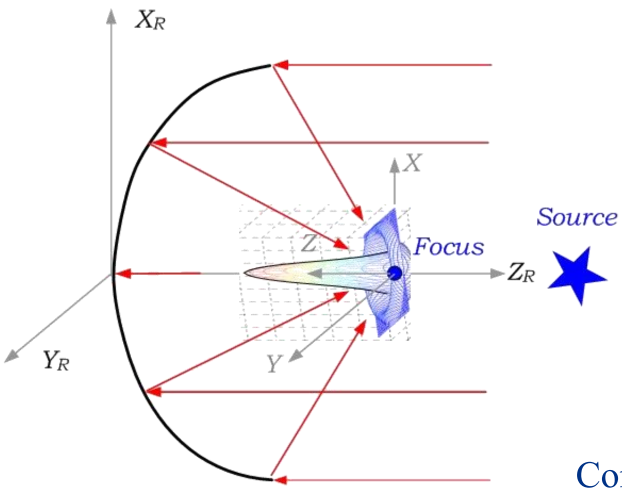

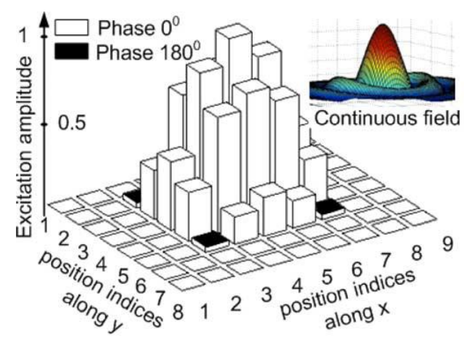

Conjugate Field Matching (CFM) approach

- Optimization of the total PAF-reflector pattern (*W. Brisken/Craeye/Veidt et, 2004*);
- Modified CFM approach with constraints on spillover (*M. V. Ivashina et., 2004*);
- Normalized CFM in combination with the black box approach (*D.Hayman, 2008*).

First experimental demonstration of 1^{st} G BFs

(CFM method with spillover control)

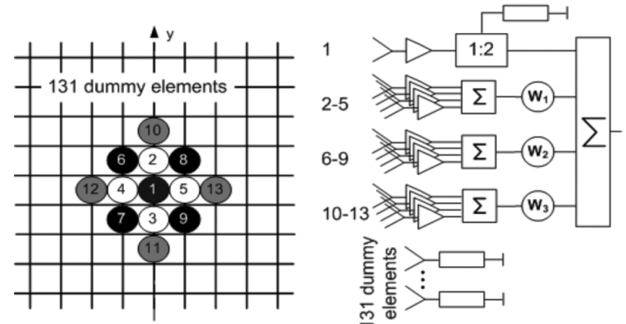

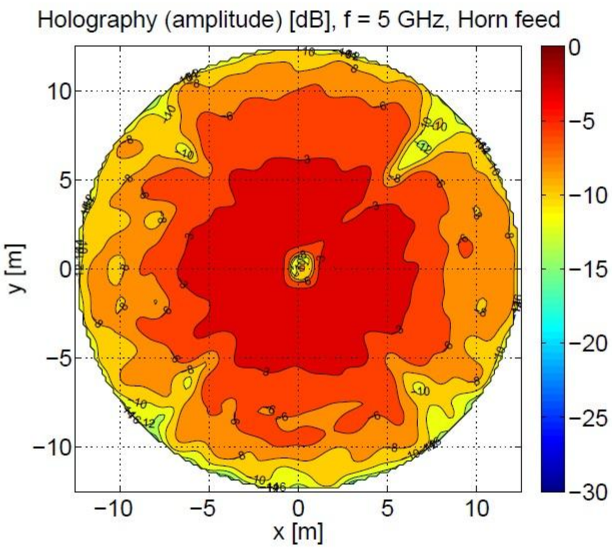

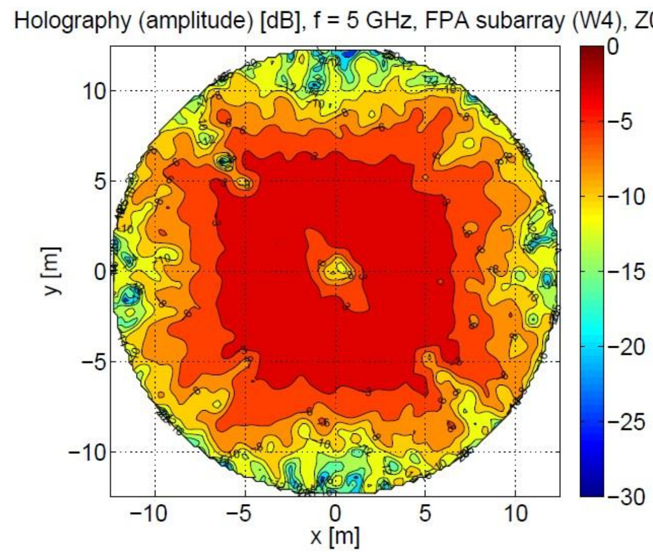

Improved illumination efficiency w.r.t conventional horn feed,
(but high receiver noise temperature)

Ivashina/van der Marel, 2005

2^{nd} G BFs: development of a theoretical framework and tools

Requires a new interdisciplinary theoretical framework involving the advanced models of the PAF antenna systems, multi-channel receivers (in the presence of coupling), and signal processing techniques.

Since 2007 - on-going activities at BYU, ASTRON/CHALMERS, DRAO, CSIRO.

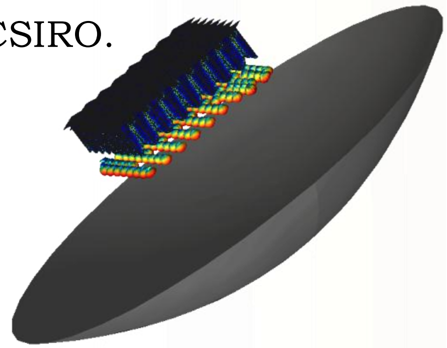

Enabling EM/MW modeling framework:

- Accurate signal-noise models of the total PAF antenna-receiver systems and practical FOMs for the purpose of optimization
  (BYU/ASTRON/CHALMERS, 2008 AWPL, 2010 IEEE TAP);

- Dedicated simulation software tools
  (CHALMERS-ASTRON, BYU, IEEE TAP, 2011).

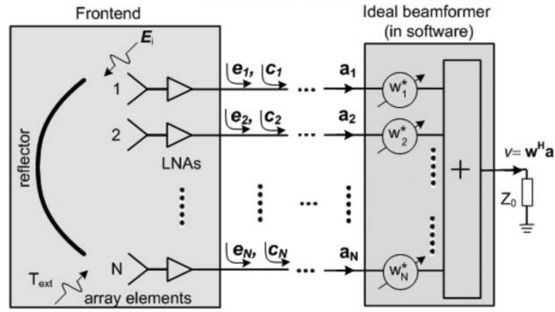

The developed mathematical methods have been implemented in the CAESAR software (Computationally Advanced and Efficient Simulator for ARrays), - a combined EM-MW simulator for the analysis of electrically large antenna array systems (Main developer is Rob Maaskant, PhD project at ASTRON, now within PostDoc at Chalmers; PAF simulator and BF optimizer – a new tool box for CAESAR developed by Ivashina/Iupikov).

2^{nd} G BFs: development of a theoretical framework and tools

Requires a new coherent interdisciplinary theoretical framework involving the advanced models of the PAF antenna systems, multi-channel receivers (in the presence of coupling), and signal processing techniques.

Since 2007 - on-going activities at BYU, ASTRON/CHALMERS, DRAO, CSIRO.

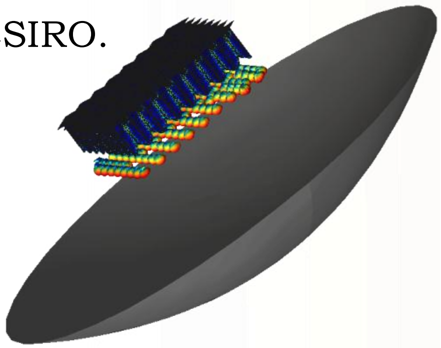

Enabling EM/MW modeling framework:

- Accurate signal-noise models of the total PAF antenna-receiver systems and practical FOMs for the purpose of optimization
  (BYU/ASTRON/CHALMERS, 2008 AWPL, 2010 IEEE TAP);

- Dedicated simulation software tools
  (CHALMERS-ASTRON, BYU, IEEE TAP, 2011).

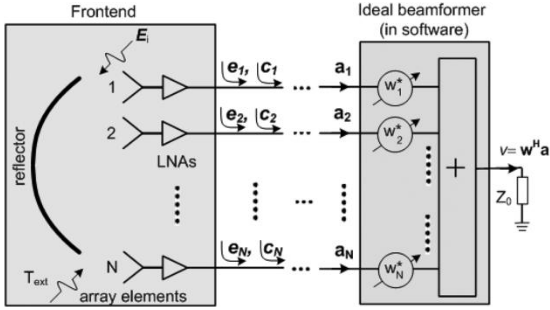

Development of dedicated algorithms:

- Using advance signal processing algorithms (van Trees) and extending these to take into account special conditions in RA signal processing (low noise, beam smoothness and stability, interference.) $\Rightarrow$ several trade-off solutions

Examples of the 2nd G BFs

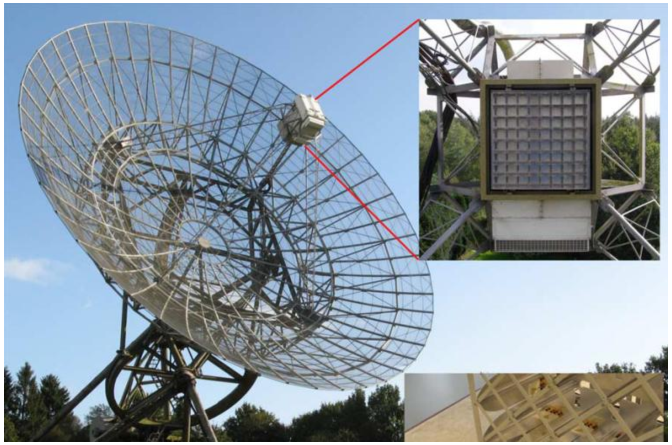

- Improved Gaussian beam fit: Error is <2% vs. <11% for maxSNR
- 1st side-lobe level was reduced from -17dB (maxSNR) to -23dB.

Trade-off between maxSNR and 'ideal' beam shape (Gaussian beam):

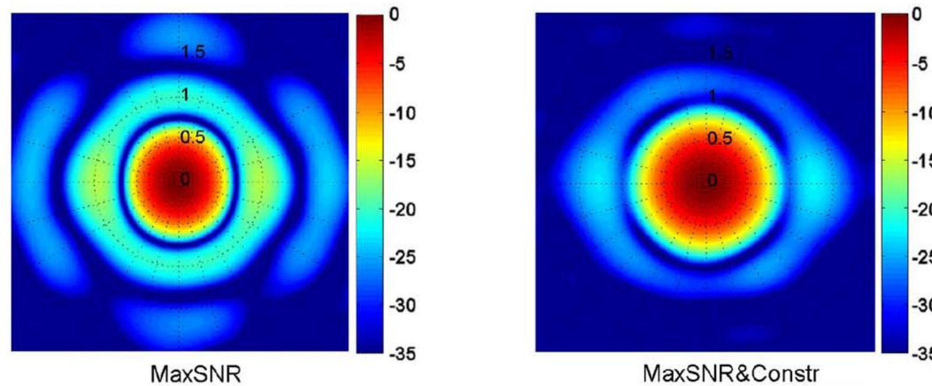

Simulated on-axis beam of APERTIF

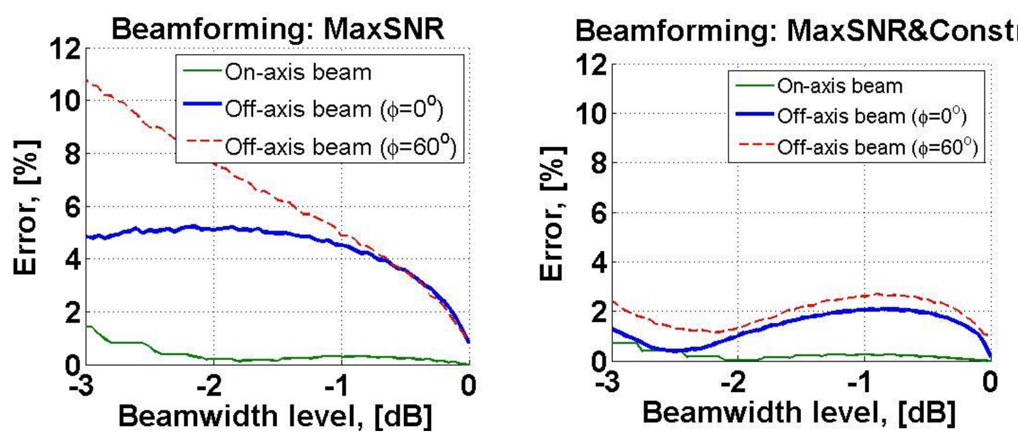

Error of the fit to the Gaussian beam

O. Iupikov et., EuCAP2011
M. Ivashina et., IEEE TAP, 2011

Examples of the 2nd G BFs

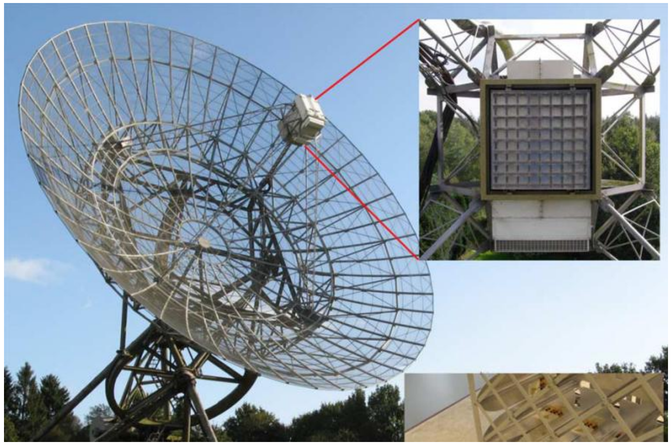

Trade-off between maxSNR and ‘ideal’ beam shape (Gaussian beam):

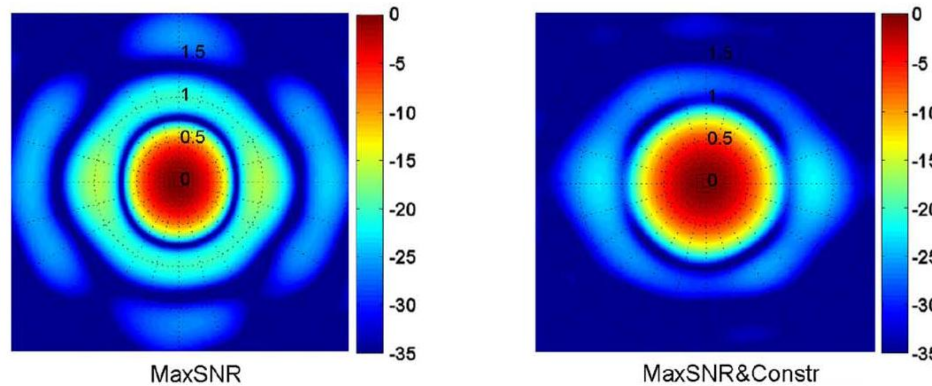

Simulated on-axis beam of APERTIF

- Improved Gaussian beam fit: Error is <2% vs. <11% for maxSNR
- 1st side-lobe level was reduced from -17dB (maxSNR) to -23dB.
- 5-20% sensitivity reduction.

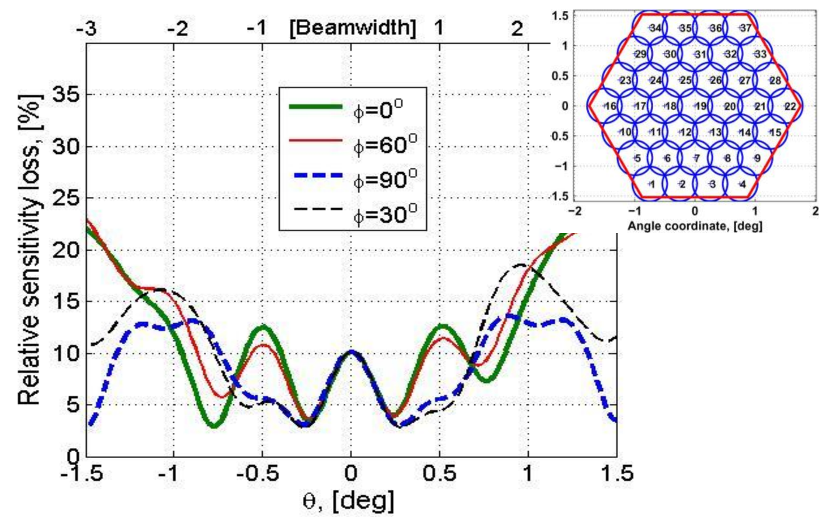

Relative sensitivity reduction

Iupikov/Ivashina.Snirnov et., EuCAP2011
M. Ivashina et., IEEE TAP, 2011

Examples of the 2^{nd} G BFs

Trade-off between maxSNR and side-lobe level:

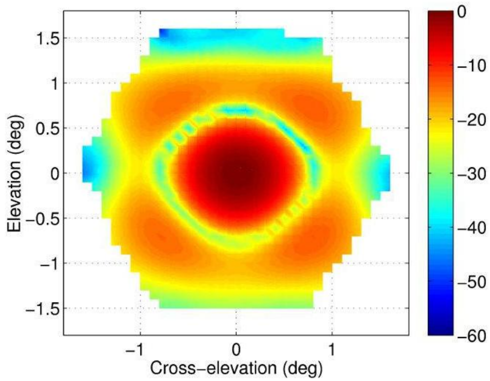

maxSNR

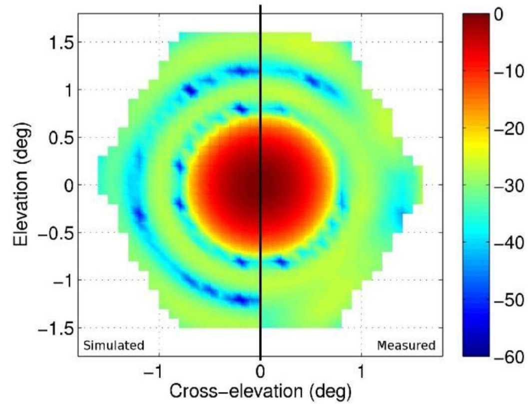

Equiripple beamformer

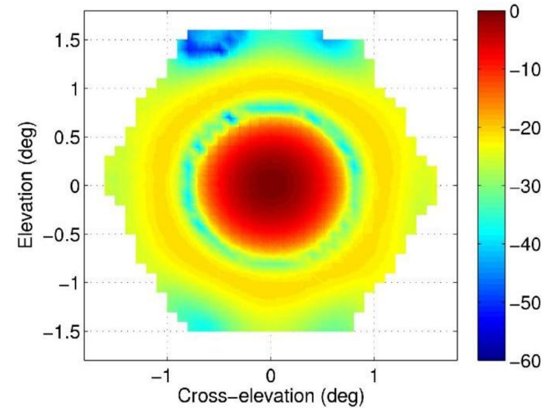

Hybrid equiripple-maxSNR

Beamformer	Beamwidth	Peak side lobes
max-SNR	$1.6°$	-13.03 dB
equiripple	$1.6°$	-26.40 dB
hybrid ($\gamma = 0.5$)	$1.6°$	-17.70 dB

The BYU/NRAO feed on the NRAO 20 meter dish.

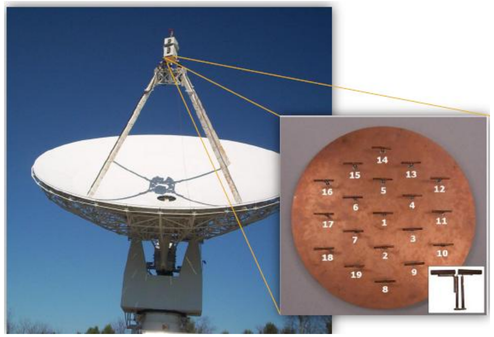

BYU
BRIGHAM YOUNG
UNIVERSITY

M. Elmer. B Jeffs, K.Warnick., International Workshop on Phased Array Antenna Systems for Radio Astronomy, May 4, 2010

Examples of the 2^{nd} G BFs

Trade-off between maxSNR and side-lobe levels:

Beamformer	Beamwidth	Peak side lobes	Sensitivity	*Sensitivity reduction*
max-SNR	$1.6°$	-13.03 dB	$2.973\ m^2/K$	
equiripple	$1.6°$	-26.40 dB	$1.839\ m^2/K$	*38%*
hybrid ($\gamma = 0.5$)	$1.6°$	-17.70 dB	$2.860\ m^2/K$	*4%*
hybrid ($\gamma = 0.25$)	$1.6°$	-21.02 dB	$2.545\ m^2/K$	*14%*

What are the effects of varying the parameter γ of constraint?

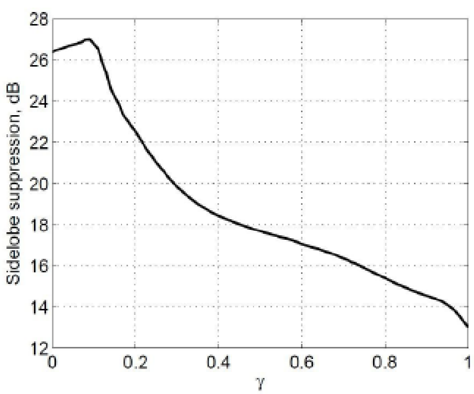

Sidelobe level, dB

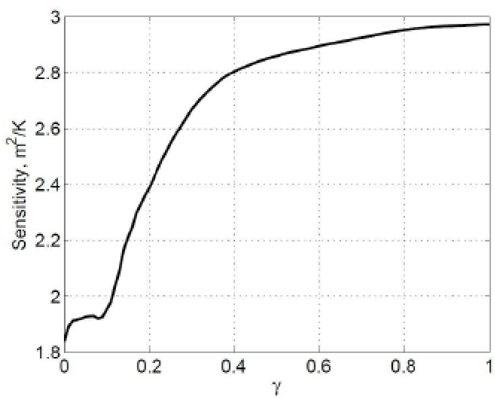

Sensitivity, m²/K

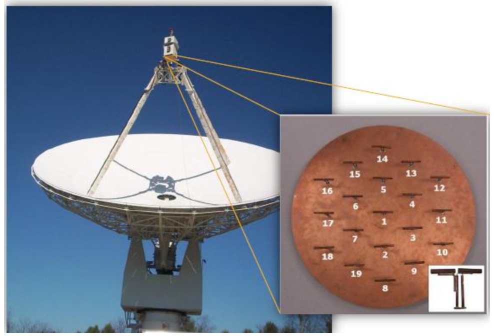

BYU
BRIGHAM YOUNG
UNIVERSITY

M. Elmer et., 2010

3^d G BFs: Polarimetric BFs

- 1^{st} and 2^{nd} G BFs are scalar beamformers.
- 3^d G BFs can provide high sensitivity and orthogonality of a polarimetric beam pair of array-based telescopes.

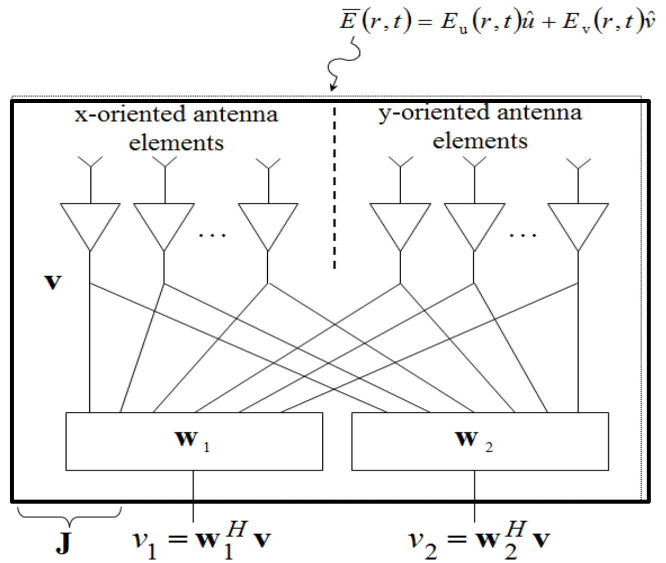

$\mathbf{R_s}$ – the covariance of the source signal in two polarizations.

$\mathbf{J}$ – describes how the input voltages in two polarizations are transformed into two polarimetric output signals.

$$\begin{bmatrix} v_1 \\ v_2 \end{bmatrix} = \underbrace{\begin{bmatrix} J_{11} & J_{12} \\ J_{21} & J_{22} \end{bmatrix}}_{\mathbf{J}} \begin{bmatrix} E_u \\ E_v \end{bmatrix}$$

If we correlate output signals v_1 and v_2, we get the beamformer output covariance matrix $\mathbf{R_o}$, which is used to reconstruct source covariance matrix $\mathbf{R'_s}$.

For an ideal system that does not introduced so-called instrumental polarization $\mathbf{J}=\mathbf{I}$.

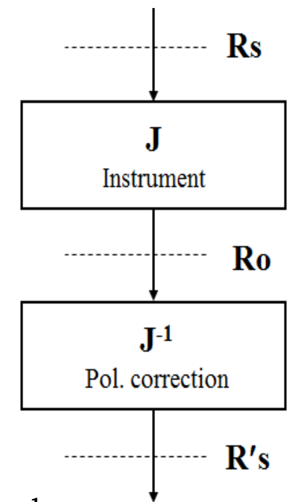

K.F. Warnick, M.V. Ivashina, S.J. Wijnholds, and R. Maaskant, 'Polarimetry with Phased Array Antennas: Theoretical Framework and Definitions', accepted for publication in *IEEE Trans. on Antennas and Propagat.*, 2011.

S.J. Wijnholds, M.V. Ivashina, R. Maaskant, T. Webb, K.F. Warnick, 'Polarimetry with Phased Array Antennas: Practical Calibration Methods', for submission to *IEEE Trans. on Antennas and Propagat.*, 2011.

CHALMERS

BYU BRIGHAM YOUNG UNIVERSITY

ASTRON Netherlands Institute for Radio Astronomy

Polarimetric beamformers

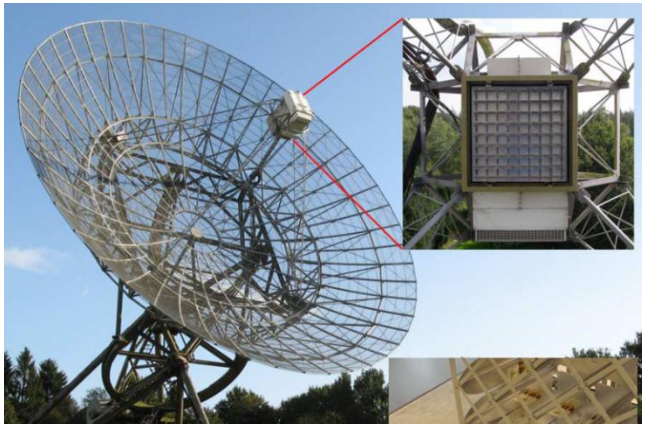

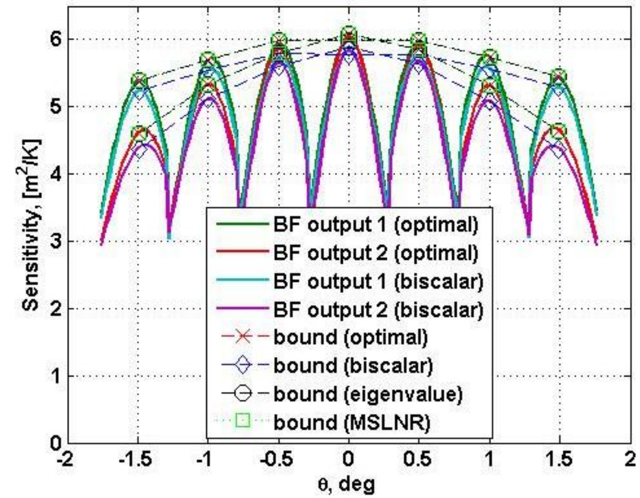

|J11| for 37 beams (optimal method)

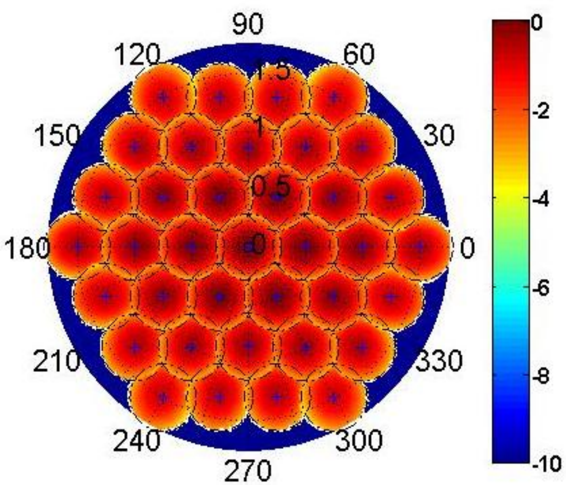

|J12| for 37 beams (optimal method)

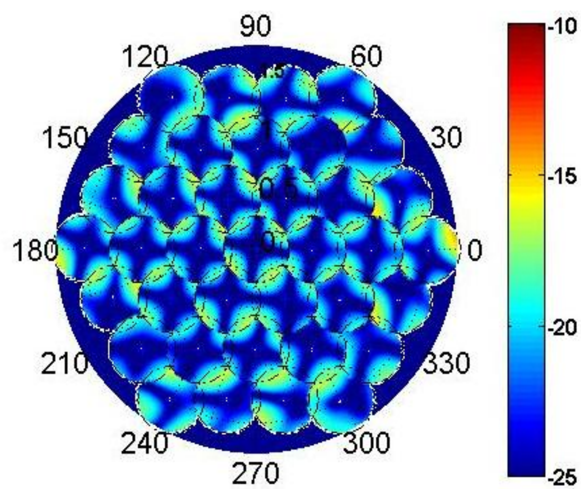

|J12| for 37 beams (bi-scalar method)

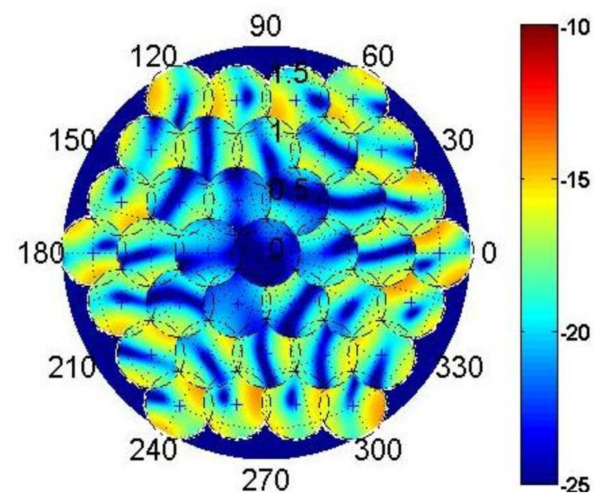

Ivashina et., URSI GASS 2011

Polarimetric homogeneity of the PAF beams is not constant over the FoV

Conclusions

PAF BFs have been developed gradually as accurate numerical models and software tools of PAF systems have become available.

The developed PAF BFs so far can be arranged in three groups.

Polarimetric BFs have been recently proposed and tested using the models of practical PAF systems.

The on-going/future work includes:

Improvement of the accuracy of the developed practical polarimetric beamformers and their experimental demonstration with on-reflector PAFs.

Development of methods for reducing the number of required telescope pointings required to calibrate all formed beams to avoid time-consuming observations of multiple sources or long observations of a single polarized source for each beam.

The temporal stability of formed beam polarization responses (Smirnov *et.*, EuCAP2011; Cappellen *et*, EuCAP2011, Wijnholds *et*, URSI GASS 2011).

References (I)

1. J. D. Kraus, *Radio Astronomy*, Second ed. Powell, OH: Cygnus-Quasar, 1986.
2. A. R. Thompson, J. M. Moran, and G. W. Swenson, Jr, *Interferometry and Synthesis in Radio Astronomy*, 2nd ed. New York: Wiley, 2001.
3. J. R. Fisher and R. F. Bradley, “Full sampling array feeds for radio telescopes,” *Proc. SPIE*, vol. 4015, pp. 308–318, 2000.
4. C. K. Hansen, K. F. Warnick, B. D. Jeffs, J. R. Fisher, and R. Bradley, “Interference mitigation using a focal plane array,” *Radio Sci.*, vol. 40, no. 5, Jun. 2005.
5. M. V. Ivashina, J. D. Bregman, and A. van Ardenne, “A way to improve the field of view of the radio-telescope with a dense focal plane array,” in *Proc. 12th Int. Crimean Conf. Microw. Telecommun. Technol.*, Sevastopol, Crimea, Ukraine, Sep. 2002, pp. 278–281.
6. M. V. Ivashina, R. Maaskant, H. van der Marel, and J.-G. bij de Vaate, “Holograpic performance verification of a focal plane array prototype,” in *Proc. 28th ESA Antenna Workshop Space Antennas Syst. Technol.*, Noordwijk, Jun. 2005, pp. 429–434.
7. B. Veidt, “The SKA memo 71, 2006: Focal-plane array architectures: Horn clusters vs. phasedarray techniques,” [Online]. Available: http:www:skatelescope:org=pages= page skares:htm
8. B. Veidt and P. Dewdney, “A phased-array feed demonstrator for radio telescopes,” in *Proc. URSI General Assembly*, 2005.
9. Ivashina, FPA Workshop, Dwingeloo, 2004.

10 D.B. Hayman, T.S. Bird, K.P. Esselle, P.J. Hall, Experimental Demonstration of Focal Plane Array Beamforming in a Prototype Radiotelescope IEEE Trans. On Antennas and Propagation, Vol. 58, No 6, June 2010.

11. W. Brisken and C. Craeye, Focal Plane Array Beam-Forming and Spill-Over Cancellation Using Vivaldi Antennas National Radio Astronomy Observatory, EVLA Memo 69, Jan. 2004 [Online]. Available http://www.aoc.nrao.edu/evla/geninfo/memoseries/evlamemo69.pdf

References (II)

12. R. Maaskant and B. Woestenburg, "Applying the active antenna impedance to achieve noise match in receiving array antennas," in Proc. IEEE AP-S Int. Symp., Honolulu, HI, Jun. 2007, pp. 5889–5892.

13. M. V. Ivashina, R. Maaskant, and B. Woestenburg, "Equivalent system representation to model the beam sensitivity of receiving antenna arrays," *IEEE Ant. Wireless Propag. Lett.*, vol. 7, pp. 733–737, 2008.

14 K. F. Warnick, B. Woestenburg, L. Belostotski, and P. Russer, "Minimizing the noise penalty due to mutual coupling for a receiving array," *IEEE Trans. Ant. Propag.*, vol. 57, no. 6, pp. 1634–1644, June 2009.

15. K. Warnick, M. Ivashina, R. Maaskant, and B. Woestenburg, "Unified Definitions of Efficiencies and System Noise Temperature for Receiving Antenna Arrays," *IEEE Transactions on Antennas and Propagation*, vol. 58, no. 6, pp. 2121–2125, 2010.

16 H. L. van Trees, *Optimum Array Processing*. New York:Wiley, 2002.

17. B. D. Jeffs and K. F. Warnick, "Signal processing for phased array feeds in radio astronomical telescopes," IEEE Trans. Signal Proc., vol. 2, no. 5, pp. 635–646, Oct. 2008.

18. M. V. Ivashina, O. Iupikov, R. Maaskant, W. A. van Cappellen, and T. Oosterloo, "An Optimal Beamforming Strategy for Wide-Field Surveys With Phased-Array-Fed Reflector Antennas", *IEEE Trans. on Aantennas Propagation*, Vol.59, Issue 6, June, 2011.

19. B. Veidt et al., "Demonstration of a dual-polarized phased-array feed," *IEEE Trans. Ant. Propag, Vol. 59, Issue 6, June, 2011.*

20. O. Iupikov, M. Ivashina, O. Smirnov, "Reducing a complexity of the beam calibration models of phased-array radio telescopes," in *Proc. EuCAP*, Rome, Italy, Apr. 2011.

21. *M. Elmer. B Jeffs, K.Warnick., 'Beamformer design methods for phased array feeds', International Workshop on Phased Array Antenna Systems for Radio Astronomy, May 4, 2010*

22. M. Ivashina, O. Iupikov, and W. van Cappellen, "Extending the capabilities of the grasp and caesar software to analyze and optimize active beamforming array feeds for reflector systems," in *Proc. ICEAA*, Sydney, Australia, 2010, pp. 197–200

Part II: Antenna Beam Modeling

Part II has been prepared by R. Maaskant and M. Ivashina (AAs) and M.Ivashina, O. Iupikov and R.Maaskant (PAFs).

References:

‘Prediction of Antenna Array Beams by Employing Only Few Physics-Based Basis-Functions and Far-Field Measurements R. Maaskant, M. V. Ivashina, S. J. Wijnholds, and K. F. Warnick.

‘Modeling the Phased Array Feed Beams Using Physics-Based Basis Functions’, M. V. Ivashina, O. A. Iupikov, R. Maaskant, S. J. Wijnholds, and K. F. Warnick.

CHALMERS

ASTRON Netherlands Institute for Radio Astronomy

BYU BRIGHAM YOUNG UNIVERSITY

Part II: Antenna Beam Modeling

Analytical Basis Functions

Examples
- *Jacobi-Bessel, Spherical Harmonics, Plane Wave Spectrum, Gaussian Beams, etc.*

Advantages
- *Set is orthogonal*
- *Continuous Functions for Interpolation*

Disadvantages
- *Contain limited physics-based information on element type, element positions, array excitations.*

Numerical Basis Functions

Examples
- *Characteristic Basis Function Patterns (CBFPs, next slides)*

Advantages
- *Physics-based basis functions (account for element type, element positioning, excitation scheme)*

Disadvantages
- *Not necessarily orthogonal*
- *Discretely sampled, thus interpolation functions needed*

Using the advantages of both methods

Hybrid Beam Modeling Approach

Hybrid and Multilevel Beam Modeling Approach

Unknown Expansion Coefficients

Reference Beam Pattern to be modeled

Numerical Basis Function Patterns (CBFPs)

$$\underline{f}(\theta,\phi) = \sum_{n=1}^{N} \alpha_n \underline{g}_n(\theta,\phi)$$

$$\underline{g}_n(\theta,\phi) = \sum_{m=1}^{M} \beta_{mn} \underline{h}_{mn}(\theta,\phi)$$

Fixed Expansion Coefficients

Analytical Basis Function Patterns

The unknown expansion coefficients α_n are determined through fitting the modeled output covariance matrix (visibilities within a station) to the measured one for at least N distinct sky reference sources

Aperture Phased Arrays (AAs)

For array antennas, the overall antenna array beam $\underline{f}$ is a weighted sum of embedded element patterns $\underline{e}_n$ (EEPs), i.e.,

$$\underline{f}(\theta,\phi)=\sum_{n=1}^{N} w_n \underline{e}_n(\theta,\phi)$$

For phased arrays with negligible edge-truncation effects, one can assume that all EEPs are identical (apart from a phase transformation):

$$\underline{e}_n(\theta,\phi)=\underline{e}_1(\theta,\phi)\exp(-\mathrm{j}\underline{k}(\theta,\phi)\cdot[\underline{r}_n-\underline{r}_1])$$

where $[\underline{r}_n-\underline{r}_1]$ is the offset position vector between element 1 and n, and $\underline{k}(\theta,\phi)=-\left(\frac{2\pi}{\lambda}\right)[\sin(\theta)\cos(\phi)\underline{\hat{x}}+\sin(\theta)\sin(\phi)\underline{\hat{y}}+\cos(\theta)\,\underline{\hat{z}}]$.

$$\underline{f}(\theta,\phi)=\underline{e}_1(\theta,\phi)\times\sum_{n=1}^{N} w_n e^{-\mathrm{j}\underline{k}(\theta,\phi)\cdot[\underline{r}_1-\underline{r}_n]}$$

Ref. Beam Pattern

Embedded Element Pattern (unknown)

Array Factor (known)

$$\underline{f}(\theta,\phi) = \underline{e}_1(\theta,\phi) \times \sum_{n=1}^{N} w_n e^{-\mathrm{j}\underline{k}(\theta,\phi)\cdot[\underline{r}_1 - \underline{r}_n]} = \underline{e}_1\,(\theta,\phi) \times AF(\underline{w},\theta,\phi)$$

The key question therefore is: how to generate a suitable set of Basis Function Patterns (CBFPs) for the smoothly varying EEP $\underline{e}_1$?

$\underline{g}_1(\theta,\phi)$

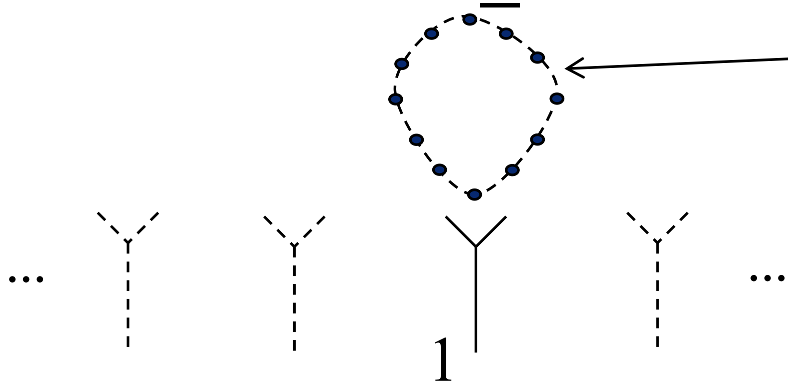

The simulated (sampled) pattern $\underline{g}_1$ can be interpolated through analytical basis functions with fixed coefficients (dashed line)

STEP 1: extract an embedded element pattern from an EM simulator (this simulated pattern will already be very close to the actual EEP as it includes array mutual coupling and the element geometry)

$$\underline{e}_1(\theta,\phi) \approx \alpha_1 \underline{g}_1(\theta,\phi)$$

$$\underline{f}(\theta,\phi) = \underline{e}_1(\theta,\phi) \times \sum_{n=1}^{N} w_n e^{-\mathrm{j}\underline{k}(\theta,\phi)\cdot[\underline{r}_1-\underline{r}_n]} = \underline{e}_1\,(\theta,\phi) \times AF\big(\underline{w},\theta,\phi\big)$$

The key question therefore is: how to generate a suitable set of Basis Function Patterns (CBFPs) for the smoothly varying EEP $\underline{e}_1$?

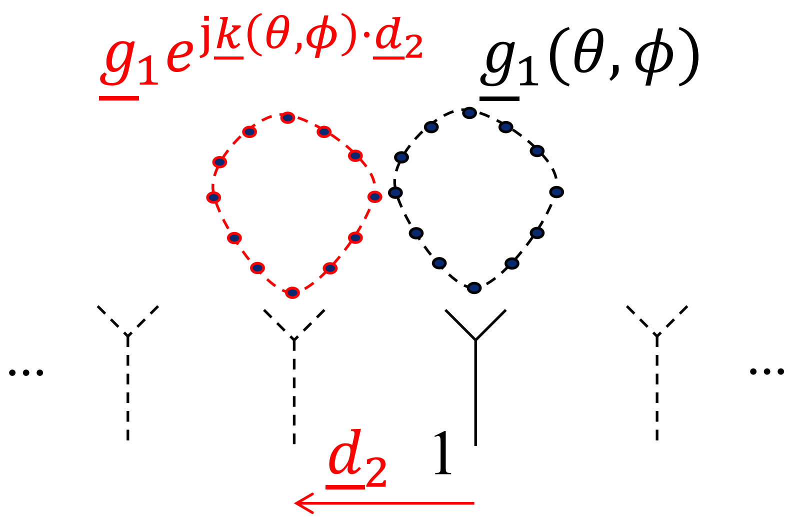

STEP 2: more than one basis function is needed for accurate modeling of the EEP. To this end, another basis function pattern is added which is derived from $\underline{g}_1$ by a geometric shift to the adjacent element

$$\underline{e}_1(\theta,\phi) \approx \alpha_1\underline{g}_1(\theta,\phi)+\alpha_2\underline{g}_1(\theta,\phi)e^{\mathrm{j}\underline{k}(\theta,\phi)\cdot\underline{d}_2}$$

$$\underline{f}(\theta,\phi) = \underline{e}_1(\theta,\phi) \times \sum_{n=1}^{N} w_n e^{-\mathrm{j}\underline{k}(\theta,\phi)\cdot[\underline{r}_1 - \underline{r}_n]} = \underline{e}_1(\theta,\phi) \times AF(\underline{w},\theta,\phi)$$

The key question therefore is: how to generate a suitable set of Basis Function Patterns (CBFPs) for the relatively smooth EEP $\underline{e}_1$?

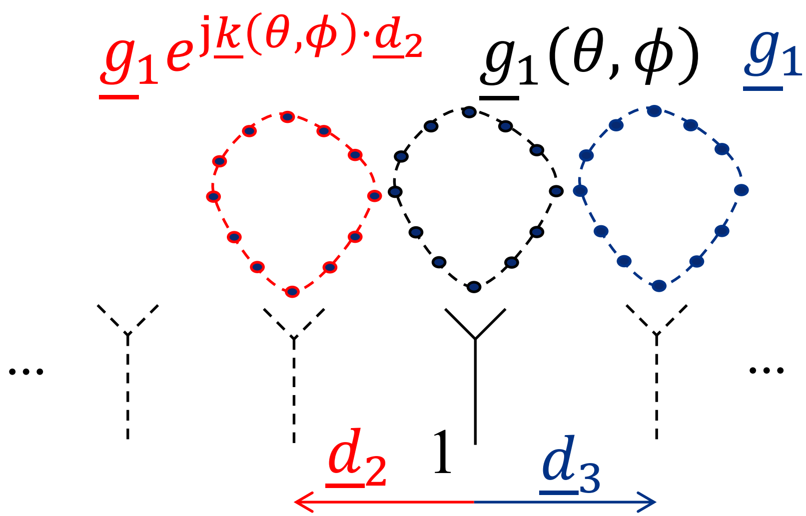

STEP 3: this procedure of "pattern shifting" is repeated until the set of basis functions is large enough for modeling the EEP sufficiently accurate

$$\underline{e}_1(\theta,\phi) \approx \alpha_1 \underline{g}_1(\theta,\phi) + \alpha_2 \underline{g}_1(\theta,\phi) e^{\mathrm{j}\underline{k}(\theta,\phi)\cdot\underline{d}_2} + \alpha_3 \underline{g}_1(\theta,\phi) e^{\mathrm{j}\underline{k}(\theta,\phi)\cdot\underline{d}_3}$$

$$\underline{e}_1(\theta,\phi) = \alpha_1 \underline{g}_1(\theta,\phi) + \alpha_2 \underline{g}_1(\theta,\phi) e^{\mathrm{j}\underline{k}(\theta,\phi)\cdot\underline{d}_2} + \alpha_3 \underline{g}_1(\theta,\phi) e^{\mathrm{j}\underline{k}(\theta,\phi)\cdot\underline{d}_3}$$

Accordingly, the embedded EEP for the nth element is modeled as

$$\underline{e}_n(\theta,\phi) = \underline{g}_1(\theta,\phi) \sum_{q=1}^{3} \alpha_q \, e^{\mathrm{j}\underline{k}(\theta,\phi)\cdot\underline{d}_n} \qquad n = 1, \dots, N$$

The final question is: how to determine the 3 pattern expansion coefficients α_1, α_2, and α_3 in practice?

STEP 4: compute the output covariance matrix using the modeled EEPs for a given sky source field and least-squares fit it to the measured one (matrix of visibilities within an AA station)

Computing the Output Voltage Covariance Matrix

The element V_{mn} of the output covariance matrix is the correlation between the mth and nth receiver output voltage, i.e.,

$$V_{mn} = v_m (v_n)^* \qquad \text{(perfectly polarized incident field, no estimation error)}$$

where the receive voltage v_n for the nth antenna element, and for the source fields $\underline{E}^i$ incident from the P distinct directions (θ_p, ϕ_p), is given as

$$v_n = C \sum_{p=1}^{P} \underline{e}_n(\theta_p, \phi_p) \cdot \underline{E}^i\,(\theta_p, \phi_p)$$

where C is a constant, and

$$\underline{e}_n(\theta, \phi) = \underline{g}_1(\theta, \phi) \sum_{q=1}^{3} \alpha_q \, e^{\mathrm{j}\underline{k}(\theta,\phi)\cdot \underline{d}_q}$$

Simulated Embedded Element Pattern, expanded in analytical basis functions

Solving for α_n

Finally, we solve for α_n by fitting the modeled output covariance matrix (V_{mn}) to the measured one ($\tilde{V}_{mn}$):

$$\epsilon = \underset{\underline{\alpha}}{\operatorname{argmin}} \left\{ \sum_{m,n} \left| \tilde{V}_{mn} - V_{mn}\left(\underline{\alpha}\right) \right|^2 \right\}$$

A more generalized description in matrix-vector form, and for unpolarized distributed sources is given in the submitted IEEE TAP paper: *R. Maaskant, M. V. Ivashina, S. J. Wijnholds, and K. F. Warnick, 'Prediction of Antenna Array Beams by Employing Only Few Physics-Based Basis-Functions and Far-Field Measurements.*

Numerical examples

Example I:
An AA of x-oriented half wavelength dipoles
- inter-element distance is 0.5λ;
- distance to the ground plane is 0.25λ

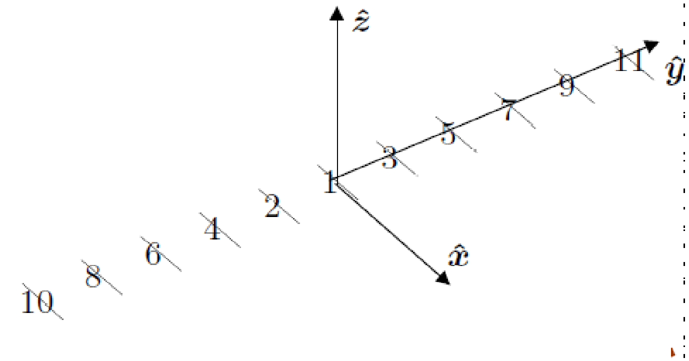

Example II:
An AA of strongly coupled array of interconnected tapered-slot antennas (TSAs) whose geometrical dimensions are similar to APERTIF and EMBRACE (an inter-element distance of 0.38λ).
.

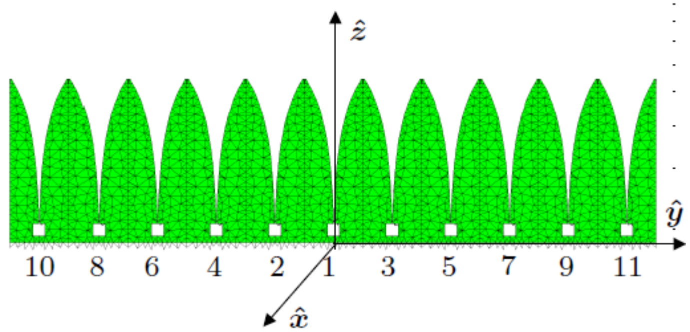

A BF scenario is a set of five x-polarized reference plane wave fields incident from $\theta = \{10^o, 20^o, 30^o, 40^o, 50^o\}$, which give rise to a rank-five voltage covariance matrix.

In the absence of measurement data of the array patterns, we have perturbed the simulated total array beam to get our ‘reference’ beam. The perturbation is accomplished by taking the short-circuited EEPs (large perturbation on the antenna loading) in place of the ideal open-circuited ones.

Error of the modeled covariance matrix

The Matlab “fminsearch” optimization routine was used for least-squared fitting. A size of the N_{act} x N_{act} covariance matrix block is varied to show the effect of including edge elements in the error minimization.

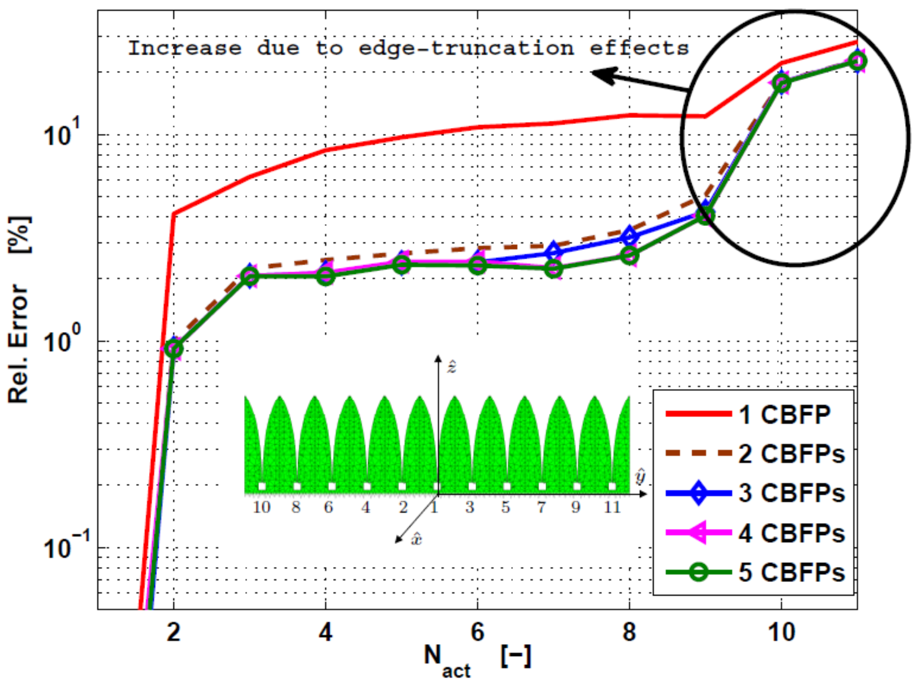

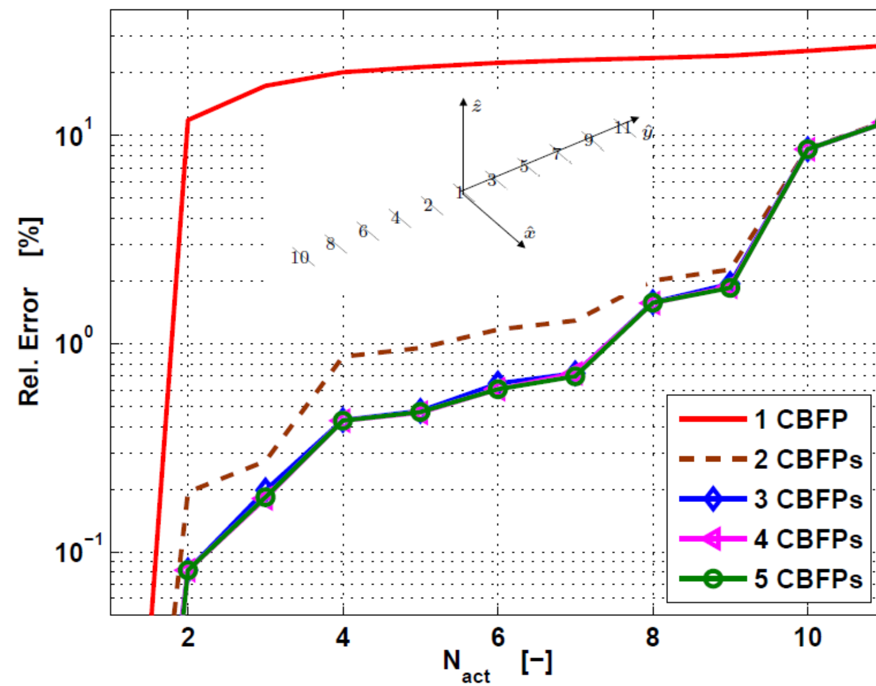

Only 3 CBFPs are needed to predict the antenna covariance matrix down to an error of about 2-3%.

However, if Nact→N (edge-element are included in the fitting), the basic assumption that all EEPs are identical ceases to hold.

The actual and modeled array beams

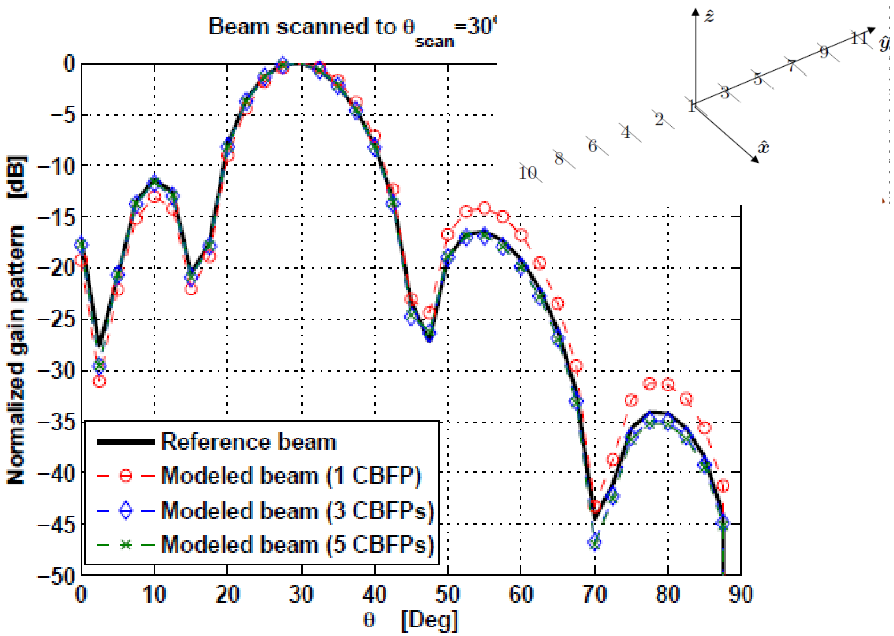

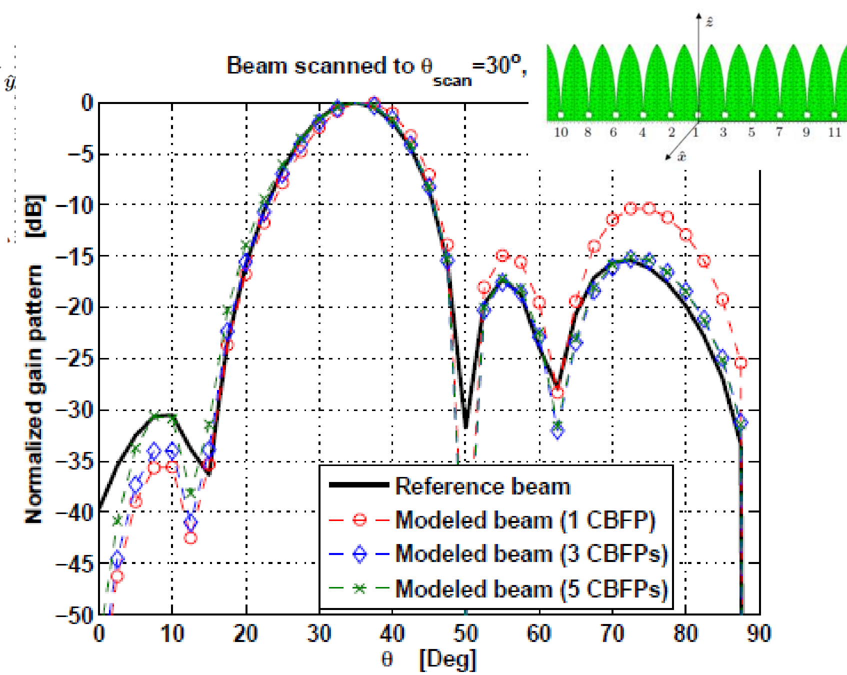

The array beam is computed from the modeled EEP as:

$$\underline{f}(\theta,\phi) = \underline{e}_1\,(\theta,\phi) \times AF\left(\underline{w},\theta,\phi\right),$$

where the EEP is modeled with 1, 3 and 5 CBFPs:

$$\underline{e}_1(\theta,\phi) \approx \alpha_1 \underline{g}_1(\theta,\phi) \qquad (1\ \text{CBFP})$$

$$\underline{e}_1(\theta,\phi) \approx \alpha_1 \underline{g}_1(\theta,\phi) + \alpha_2 \underline{g}_1(\theta,\phi) e^{j\underline{k}(\theta,\phi)\cdot\underline{d}_2} + \alpha_3 \underline{g}_1(\theta,\phi) e^{j\underline{k}(\theta,\phi)\cdot\underline{d}_3} \quad (3\ \text{CBFP})$$

The actual and modeled array beams

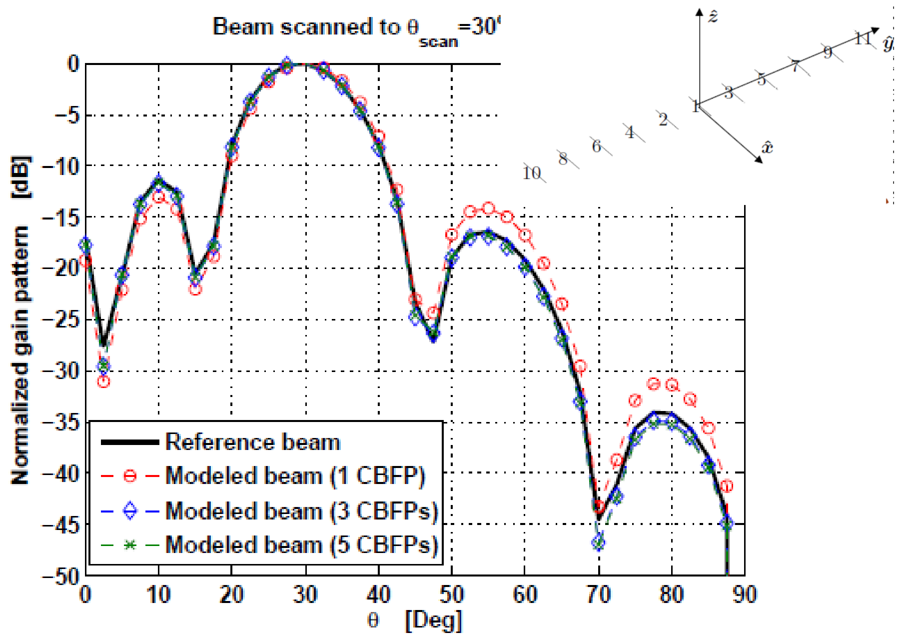

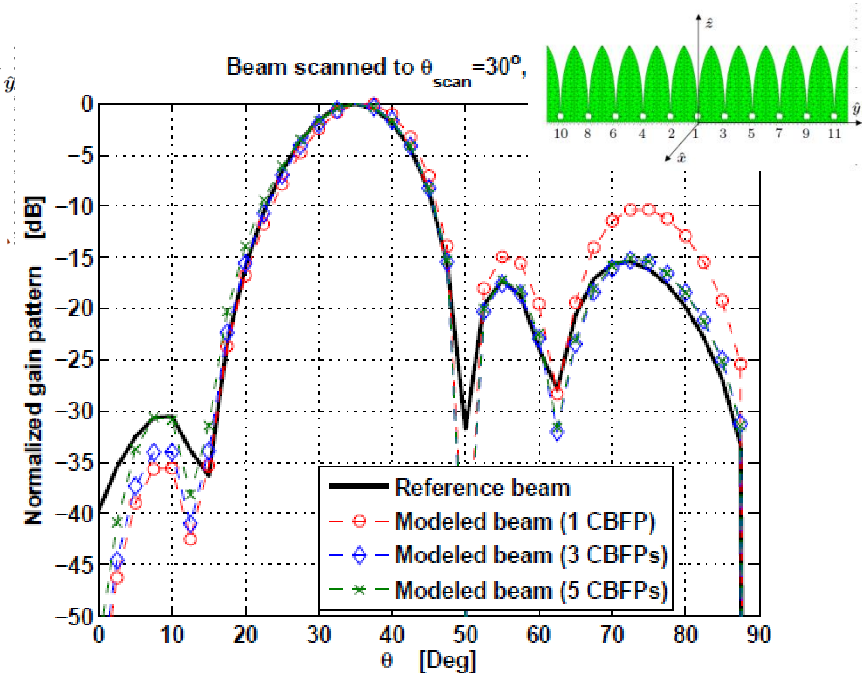

The gain pattern difference, computed relative to the maximum pattern gain

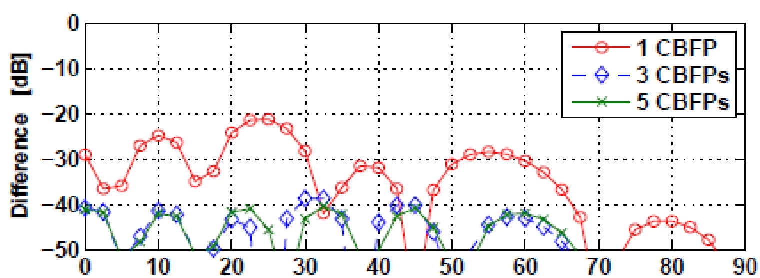

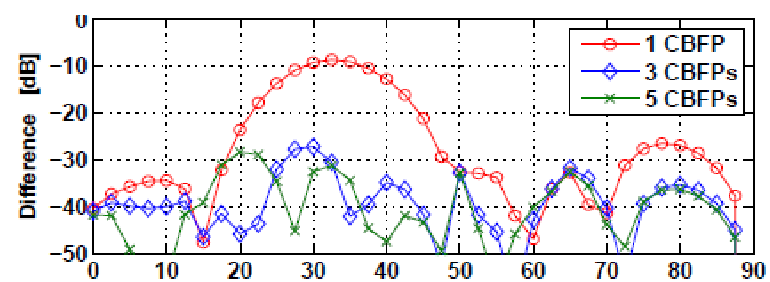

By employing only 3 CBFPs, the RLGD is smaller than -40dB for the dipole array, and -30dB for the TSA array, over the entire range of observation angles. Increasing the number of CBFPs does not improve the accuracy, because we have reached the point beyond which the EEPs cannot be regarded identical anymore.

Extension of the beam modeling concept to PAFs

The considered methods are based on the same beam modeling concept as that for AAs.

- Method I (approximate method):
  approximate modeling of the EEPs of the PAF after reflection from the dish.

- Method II (proposed method):
  modeling of the EEPs of the PAF feed (without reflector) and then calculating the corresponding EEPs on the sky with a reflector EM simulator.

Numerical example:

Reflector antenna (F/D=0.35, D=25m) with a linear array of 11 dipole antennas (inter-element separation is 0.5λ, 1GHz).

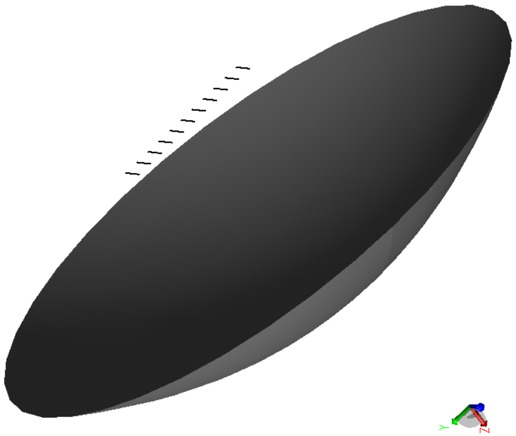

Method 1 (approximate method):

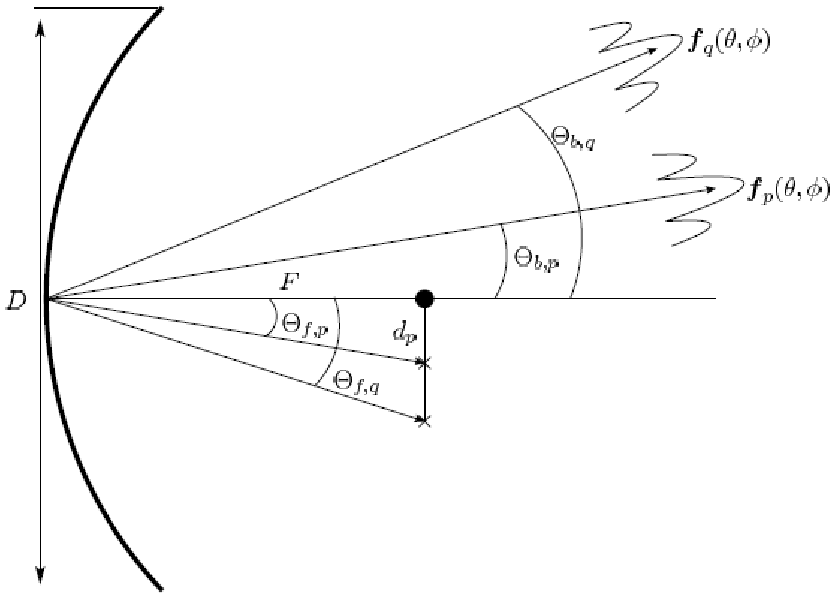

$$\mathrm{BDF}_p = \frac{\Theta_{b,p}}{\Theta_{f,p}} = \frac{\sin^{-1}\left(\frac{d_p}{F}\frac{k+(4F/D)^2}{1+(4F/D)^2}\right)}{\tan^{-1}(d_p/F)}$$

Each shift follows from the beam deviation factor, where we can use the locations of the nearest neighboring antennas as lateral displacements in the focal plane.

Assumption: All EEPs, defined after scattering from the reflector, are the same, apart from the beam deflection angle $\Theta_{b,p}$. (This does not hold for edge elements, but these have a negligible contribution to the beamforming for most formed beams.)

Each EEP can be expanded into the same set of CBFPs:

- The primary CBFP is the simulated (or a priori measured) EEP of the element located closest to the focal point of the reflector;

- The secondary CBFPs are derived from the primary CBFP by applying angular shifts to this basis function.

Approximate method: generation of CBFPs

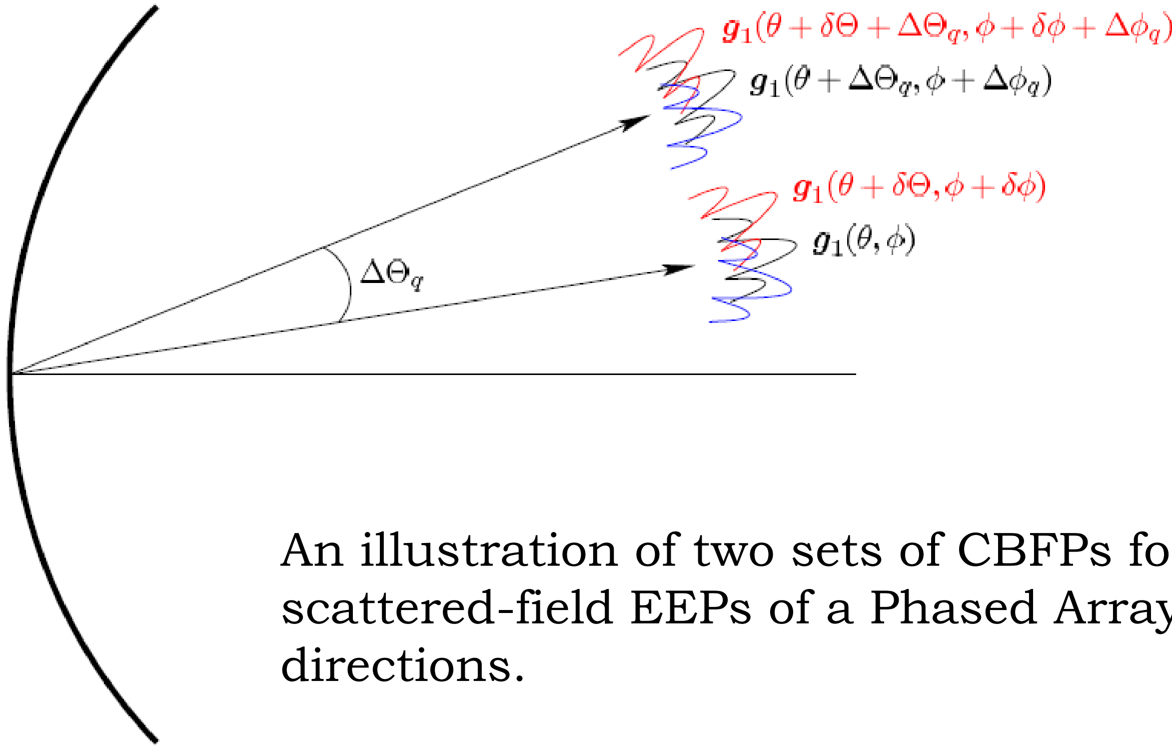

An illustration of two sets of CBFPs for modeling the scattered-field EEPs of a Phased Array Feed (PAF) in two directions.

$\{\delta\theta_m, \delta\phi_m\}$ are the angular shifts between CBFPs within the same set,

$\{\Delta\theta_q, \Delta\phi_q\}$ are the angular shifts between sets of CBFPs.

Some results for Method I

Reference beam is the non-perturbed simulated on-axis PAF beam; modeled beam is computed employing 1 CBF

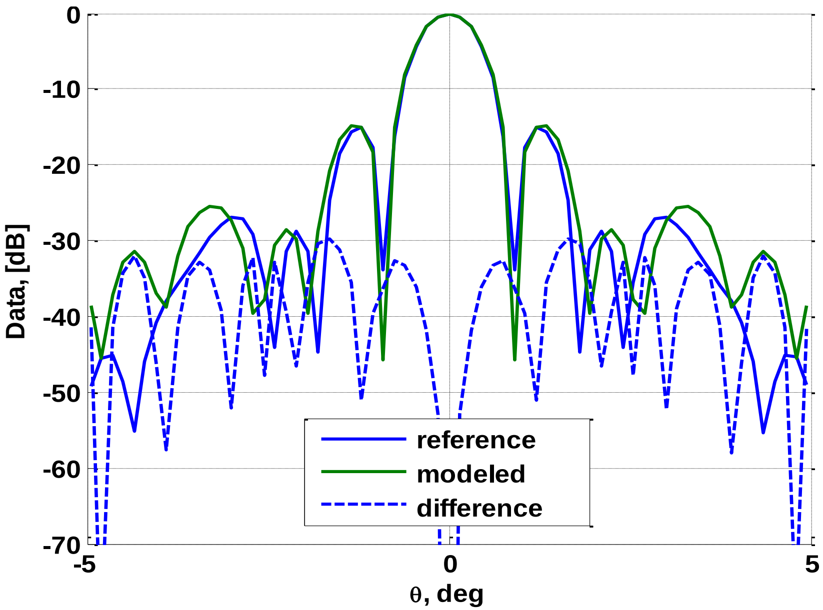

Reference is the perturbed simulated off-axis beam (gain drifts ±0.5dB and ±5°); modeled beam is computed employing 1 CBF

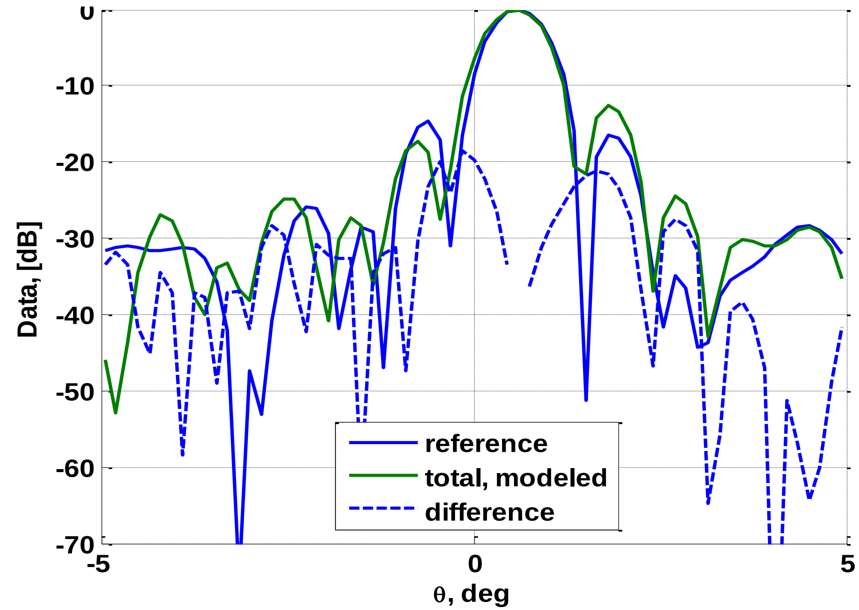

Summary: For 1-3 CBFPS, the relative error of the modeled covariance matrix is ~10% , and the resulting modeled array beams match the reference ones within the main lobe and first side lobes only.

An improvement is possible, but at the cost of a significant increase of the CBFPs. Main reason is a dominant effect of reflector (phase aberrations) on the shapes of EEPs for feed elements, which are laterally displaced from the focal point.

Method II:

Step 1: Model the EEPs of the PAF (before scattering from the dish) in the same way as for the AA:

$$\underline{e}_n(\theta,\phi) = \underline{g}_1(\theta,\phi) \sum_{q=1}^{Q_{CBFPs}} \alpha_q \, e^{\mathrm{j}\underline{k}(\theta,\phi)\cdot\underline{d}_n}$$

where $\underline{g}_1(\theta,\phi)$ has been extracted from an EM simulator.

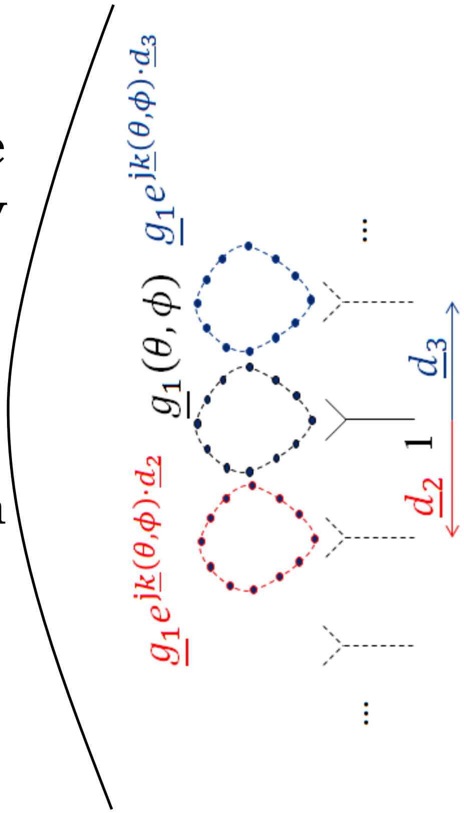

Method II:

Step 1: Model the EEPs of the PAF (before scattering from the dish) in the same way as for the AA:

$$\underline{e}_n(\theta,\phi) = \underline{g}_1(\theta,\phi) \sum_{q=1}^{Q_{CBFPs}} \alpha_q \, e^{\mathrm{j}\underline{k}(\theta,\phi)\cdot\underline{d}_n}$$

where $\underline{g}_1(\theta,\phi)$ has been extracted from an EM simulator.

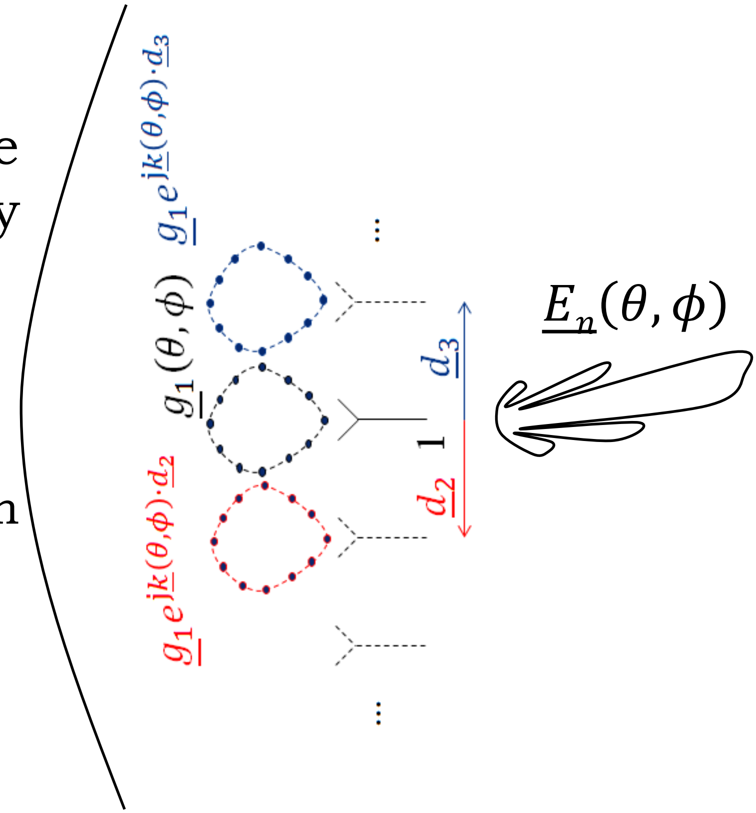

Step 2: Compute from array EEPs $e_n\ (\theta,\phi)$ (n=1,2,…,N) the corresponding EEP after scattering from the dish $E_n(\theta,\phi)$ with an EM reflector simulator. Using these patterns, we can determine the coefficients $\alpha_1, \alpha_2, \ldots, \alpha_{Q_{CBFPs}}$ by fitting the moddeled covariance matrix to the measured one.

Method II:

Step 1: Model the EEPs of the PAF (before scattering from the dish) in the same way as for the AA:

$$\underline{e}_n(\theta,\phi) = \underline{g}_1(\theta,\phi) \sum_{q=1}^{Q_{CBEPs}} \alpha_q \, e^{\mathrm{j}\underline{k}(\theta,\phi)\cdot \underline{d}_q}$$

where $\underline{g}_1(\theta,\phi)$ has been extracted from an EM simulator.

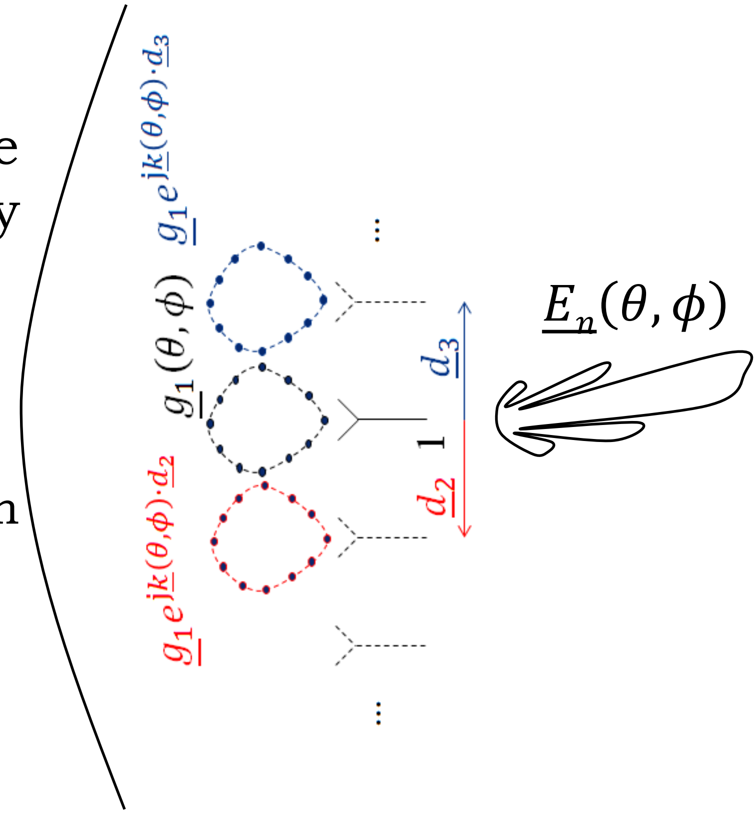

Step 2: Compute from array EEPs $e_n\,(\theta,\phi)$ (n=1,2,…,N) the corresponding EEP after scattering from the dish $\underline{E}_n(\theta,\phi)$ with an EM reflector simulator.

Step 3: Calculate the total PAF-reflector antenna beam, using the known beamformer weight vector $\underline{\mathrm{w}}$ and modeled EEPs $\underline{E}_n(\theta,\phi)$.

$$\underline{F}_n(\theta,\phi) = \sum_{n=1}^{N} \underline{E}_n(\theta,\phi) w_n$$

Method II: Initial numerical results

Only 3 CBFPs are needed to predict the antenna covariance matrix down to an error of about 4-5%.

The reference pattern, which is obtained using the simulated EEPs, is perturbed by introducing electronic gain variations (±0.5dB and ±5º); The modeled pattern is computed by employing 3 CBFPs.

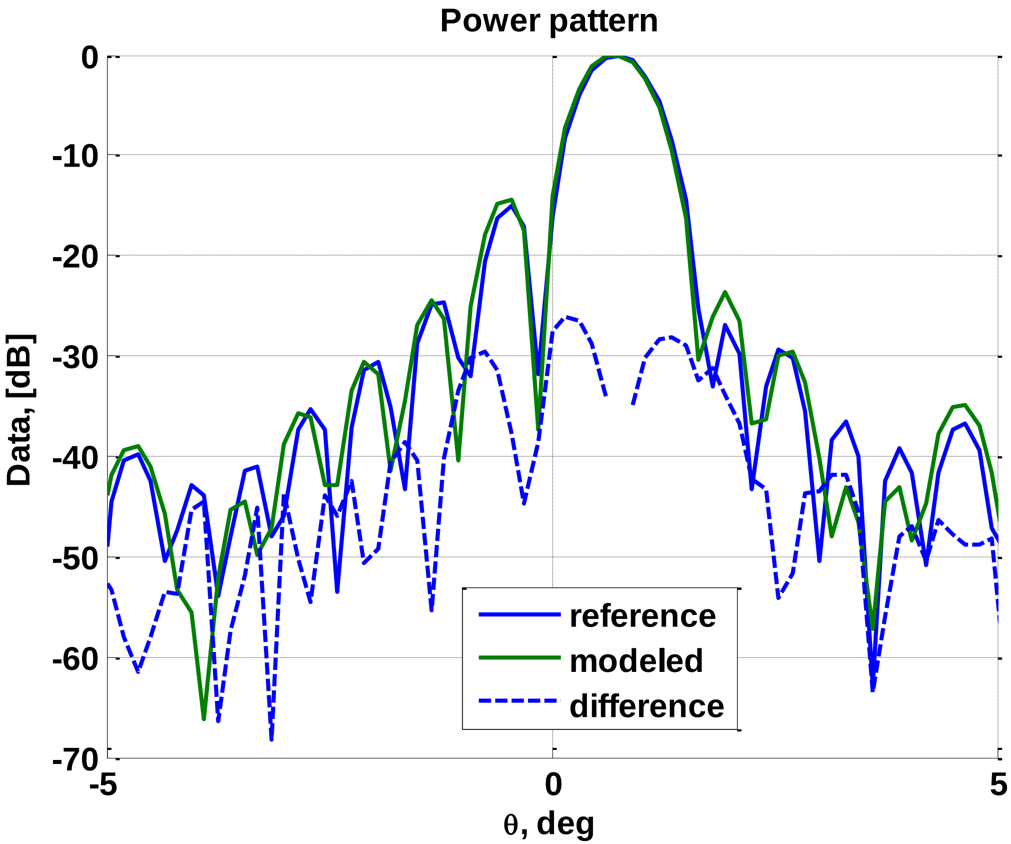

The gain difference has been found to be small for all lobes and beam scan angles.

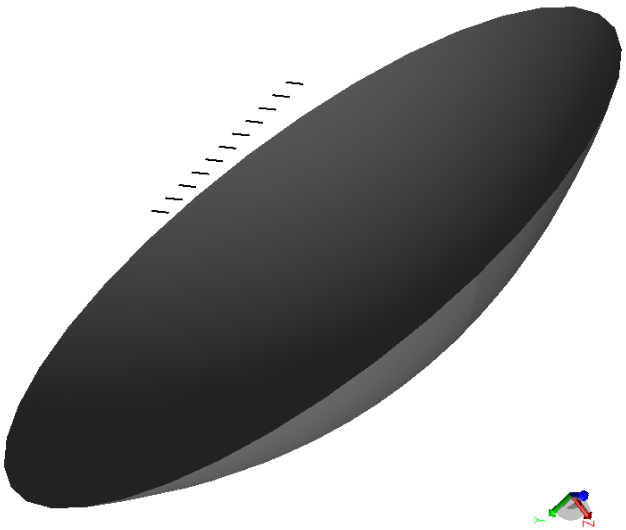

More results

The reference pattern, which is obtained using the simulated EEPs, is perturbed by setting the gain of element #5 or #7 to set to zero (broken channel); The modeled pattern is computed by employing 3 CBFPs.

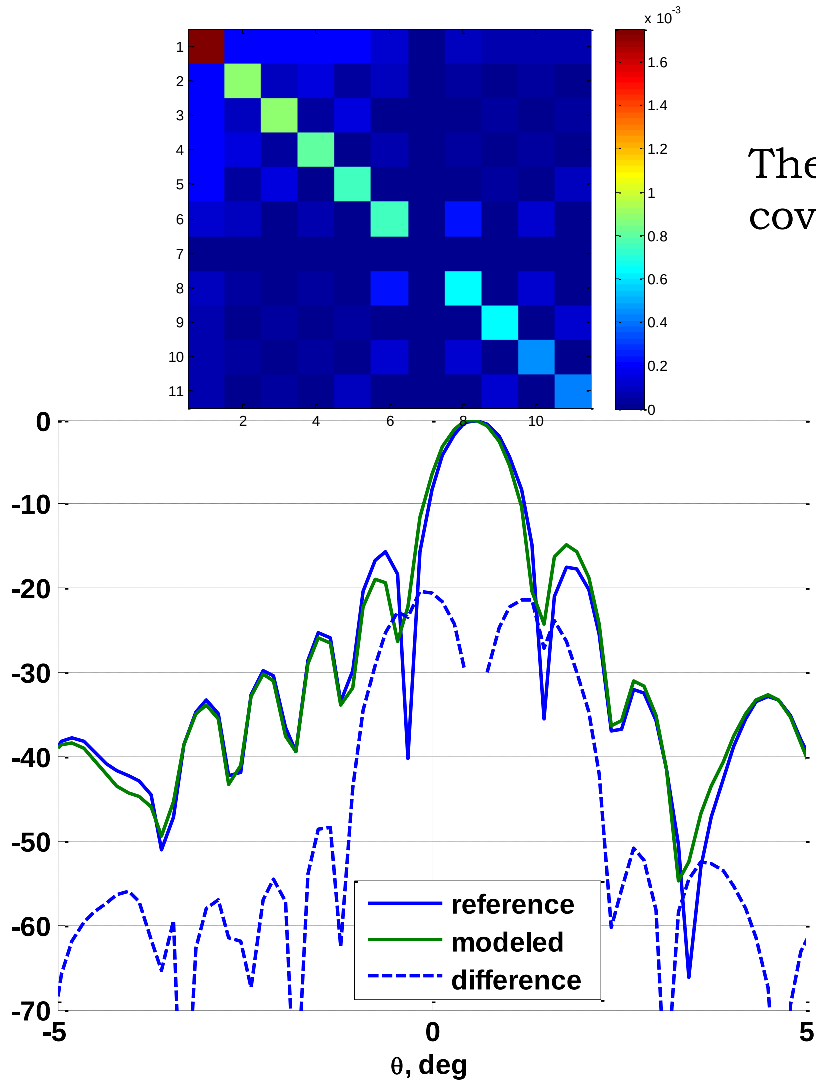

The reference output covariance matrices

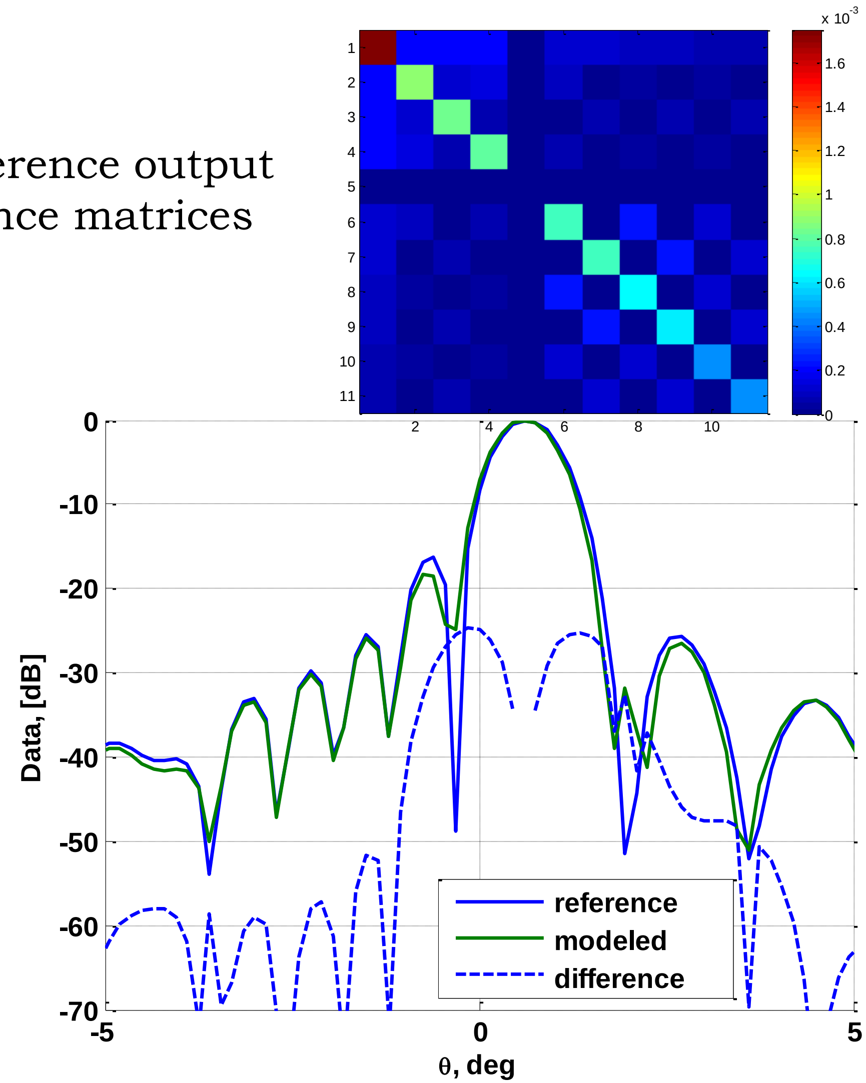

Simulated and Measured PAF beams:

The existing PAF simulation tools deliver the PAF beams which are well matched to the measured beams obtained with actual PAF systems (Examples include BYU PAF system and APERTIF).

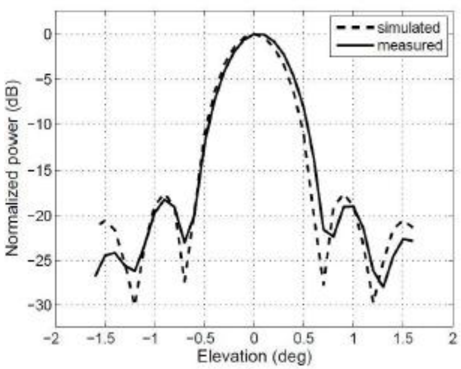

(a) Power pattern of array element 1.

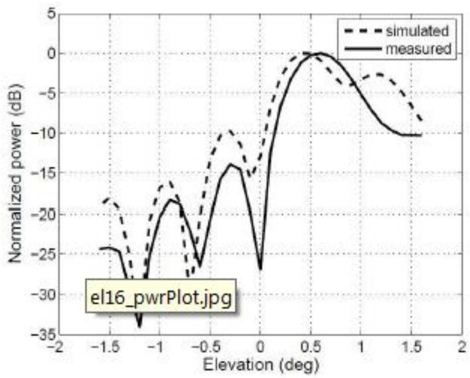

(b) Power pattern of array element 16.

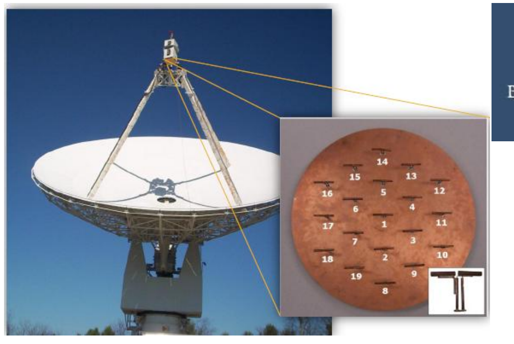

BYU
BRIGHAM YOUNG
UNIVERSITY

M. Elmer. B Jeffs, K.Warnick., Int.Workshop on Phased Array Antenna Systems for RA, May , 2010

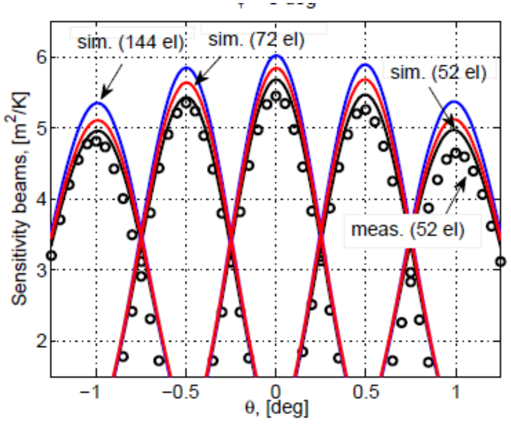

Measurement data for APERTIF system was provided by W. van Cappellen.
More comparison results are available (see Ivashina et. ICEAA2010 and IEEE TAP 2011)

Conclusions (I):

1. A multi-level hybrid beam modeling approach has been proposed and demonstrated for AA and PAF numerical examples. It shows that only 3 CBFPs are sufficient to model the array beam well: the accuracy is good both for main beam and side lobes. The expansion coefficients can be determined in practice from the measured receiver output covariance matrix (block).

2. Our findings for AAs are in line with observations of C.Craeye *et*, (CALIM, Aug. 2011) that a small number of basis functions is sufficient.

3. Future studies: to apply the proposed method in resolving the unitary matrix ambiguities for unpolarized sources.

Conclusions (II):

1. The proposed multi-level hybrid approach fits well into the MeqTrees paradigm, which is general enough to accommodate both analytic and empirical basis functions, or any combination of these. This means that rather than employing analytical basis function patterns alone, MeqTrees could invoke the EM solver first to find a relatively small deterministic set of numerically-generated physics-based basis function patterns. After that, MeqTrees could model each of these basis function patterns by analytical basis functions (as usually done for interpolation purposes).

2. We are happy to contribute to the development of MeqTrees through a collaborative effort for including this new functionality!

Acknowledgement

CHALMERS: Rob Maaskant, Oleg Iupikov, Tobia Carozzi;

ASTRON: Stefan Wijnholds, Wim van Cappellen, Oleg Smirnov;

BYU: Karl Warnick, Brian Jeffs, Mike Elmer;

To the 3GC-II organizers for a great opportunity to give this talk!!!

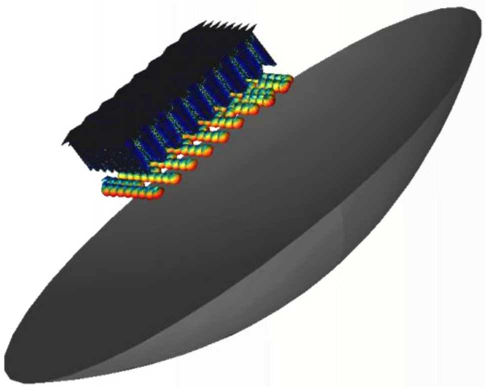

CAESAR software (Computationally Advanced and Efficient Simulator for ARrays), and the PAF simulator toolbox are dedicated software tools for phased-array radio telescopes.